



HAL
open science

Tailored glycosylated anode surfaces Addressing the exoelectrogen bacterial community via functional layers for microbial fuel cell applications

Alessandro Iannaci, Adam Myles, Thomas Flinois, James A Behan, Frédéric Barrière, Eoin M. Scanlan, Paula E Colavita

► To cite this version:

Alessandro Iannaci, Adam Myles, Thomas Flinois, James A Behan, Frédéric Barrière, et al.. Tailored glycosylated anode surfaces Addressing the exoelectrogen bacterial community via functional layers for microbial fuel cell applications. *Bioelectrochemistry*, 2020, 136, pp.107621. 10.1016/j.bioelechem.2020.107621 . hal-02930243

HAL Id: hal-02930243

<https://hal.science/hal-02930243>

Submitted on 30 Sep 2020

HAL is a multi-disciplinary open access archive for the deposit and dissemination of scientific research documents, whether they are published or not. The documents may come from teaching and research institutions in France or abroad, or from public or private research centers.

L'archive ouverte pluridisciplinaire **HAL**, est destinée au dépôt et à la diffusion de documents scientifiques de niveau recherche, publiés ou non, émanant des établissements d'enseignement et de recherche français ou étrangers, des laboratoires publics ou privés.



Tailored glycosylated anode surfaces: Addressing the exoelectrogen bacterial community via functional layers for microbial fuel cell applications

Alessandro Iannaci^a, Adam Myles^a, Thomas Flinois^b, James A. Behan^a, Frédéric Barrière^{b,*}, Eoin M. Scanlan^{a,*}, Paula E. Colavita^{a,*}

^a School of Chemistry, CRANN and AMBER Research Centres, Trinity College Dublin, College Green, Dublin 2, Ireland

^b Univ Rennes, CNRS, Institut des Sciences Chimiques de Rennes - UMR 6226, F-35000 Rennes, France

ARTICLE INFO

Article history:

Received 1 May 2020

Received in revised form 21 July 2020

Accepted 23 July 2020

Available online 27 July 2020

ABSTRACT

Grafting of aryldiazonium cations bearing a *p*-mannoside functionality over microbial fuel cell (MFC) anode materials was performed to investigate the ability of aryl-glycoside layers to regulate colonisation by biocatalytic biofilms. Covalent attachment was achieved via spontaneous reactions and via electrochemically-assisted grafting using potential step experiments. The effect of different functionalisation protocols on MFC performance is discussed in terms of changes in wettability, roughness and electrochemical response of modified electrodes. Water contact angle measurements (WCA) show that aryl-mannoside grafting yields a significant increase in hydrophilic character. Surface roughness determinations via atomic force microscopy (AFM) suggest a more disordered glycan adlayer when electrografting is used to facilitate chemisorption. MFCs were used as living sensors to successfully test the coated electrodes: the response of the MFCs in terms of start-up time was accelerated when compared to that of MFC equipped with non-modified electrodes, this suggests a faster development of a mature biofilm community resulting from aryldiazonium modifications, as confirmed by cyclic voltammetry of MFC anodes. These results therefore indicate that modification with glycans offers a bioinspired route to accelerating biofilm colonisation without any adverse effects on final MFC outputs.

© 2020 The Authors. Published by Elsevier B.V. This is an open access article under the CC BY license (<http://creativecommons.org/licenses/by/4.0/>).

1. Introduction

The discovery of electroactive microorganisms by Potter in 1911 [1,2] opened new frontiers in alternative energy technologies and environmental chemistry and led to the development of Microbial Fuel Cells (MFCs). MFCs and related microbial bioelectrochemical systems, such as plant microbial fuel cells and microbial electrolysis cells, are some of the most interesting energy conversion devices with potential to facilitate the transition to a green economy. MFCs can generate electrical power using low-value bio-resources as fuels, e.g. wastewater, via bio-catalytic processes at room temperature thus transforming a waste management problem into a high-value product [3,4].

Colonisation of electrodes by suitable bacterial consortia and effective biofilm-electrode coupling are critical for the success of MFC devices and bioelectrochemical systems in general [5–8]. Therefore, approaches aimed at selecting for robust bacterial com-

munities and improving biofilm-electrode coupling have been the subject of intense investigation for the effective development of bioelectrochemical technologies and their further implementation beyond the laboratory [3,9,10]. Interfacial modifications of solid electrodes are particularly interesting to address this challenge, as they offer the possibility of tailoring the electrode surface to enhance charge transfer rates while preserving the bulk mechanical/conducting properties of the solid electrode material. Recent examples of interfacial electrode modifications explored include the use of inorganic nanoparticles and nanocarbons [6,8,11], nanopatterning and nanoroughness modifications [12], ionic liquids [13] and conductive polymers [8,14].

Carbon-based materials are widely used as bioanode materials because of their high conductivity, good stability and low cost, hence a variety of strategies have been investigated to improve their performance. For instance, tuning of carbon morphology to achieve high surface area can enhance power densities; this has been ascribed to faster colonisation times and reductions in fouling, as suggested by several groups [12,15–18]. Surface grafting with composites based on polyaniline/carbon allotropes demonstrates electron transfer promotion and better adhesion between

* Corresponding authors.

E-mail addresses: frederic.barriere@univ-rennes1.fr (F. Barrière), scanlae@tcd.ie (E.M. Scanlan), colavitp@tcd.ie (P.E. Colavita).

biofilm and anode surface [19–21]. Chemical modifications of the carbon surface via oxidative treatments have also been observed to result in increased power densities [22–26]; improvements are generally attributed to enhanced adhesion and growth of the biofilm after introduction of hydrophilic oxidised groups, although chemical effects are often coupled with changes in morphology caused by oxidative etching [26,27]. Thermal treatment in ammonia atmosphere of graphite and carbon felts has been similarly found to improve performance [25,28].

Surface modification reactions that result in immobilisation of chemical moieties without affecting carbon morphology are of particular interest as they can be leveraged to investigate the role of interfacial functional groups on biofilm development and on the regulation of its coupling to the electrode surface. Functionalisation using aryldiazonium salts [29] offers such a possibility: aryldiazonium cations bearing a variety of functions can react under mild conditions via spontaneous or electrochemically assisted reactions from solution, yielding covalently attached moieties on carbons [30–35], as illustrated in Fig. 1 for the specific cations used in this work. Picot et al. [33] used this methodology to investigate the effect of functional groups including amine, carboxylate and triphenylphosphonium on the performance of MFC anodes. They found that the functional group net charge and hydrophilicity can affect charge transfer at the bio-electrode interface; importantly, they observed that the functional group affected the diversity in the biofilm. This group as well as others [36–38] have observed that anode surface pre-modification through electrografting of aryldiazonium bearing a *p*-amino functionality results in increased power densities, although careful control of molecular coverage is necessary to maintain fast charge transfer to the carbon electrode. Finally, a unique advantage offered by aryldiazonium chemistry is that of enabling the immobilisation of functional groups to explore specific affinity interactions with electroactive

microorganisms. For instance, immobilisation of phenylboronic acid groups was used to target affinity binding interactions of these moieties with lipopolysaccharide diols in bacterial membranes, and resulted in significantly faster start-up times after the adlayer thickness was optimised [32]. More recently, diazopyridinium cations were used to investigate whether immobilised pyridine could mediate charge transfer between the electrode and the heme groups of *c*-type cytochromes in the biofilm, as is the case for cytochromes in solution [30].

In this work we investigate, for the first time, the application of aryldiazonium salts bearing glycan functionalities for the modulation of MFC bioanode performance. Glycans are known to regulate specific and non-specific interactions in nature and are involved in a wide range of biological functions, including control of conformational stability, cell recognition, cell adhesion, infection and biofilm formation. Past work from our group has shown that aryldiazonium cations bearing glycosides can be used to prepare functional layers of mono- and di-saccharides on carbon and other substrates [39–43]. Interestingly, we observed that these saccharide adlayers reduce unspecific protein adsorption as well as retention of foulants in a range of complex biomass-rich media [42–44]. This behaviour can be attributed to the ability of glycans to inhibit unspecific binding, similar to the glycocalyx that surrounds and protects many cells. However, glycans can also display specific binding interactions with lectins which promote bacterial adhesion and attachment through recognition events at fimbriae and pili [45–47]. For instance, mannose, galactose, fucose, glucosamine and sialic acid units are all known to signal bacterial adhesion and promote surface colonisation. This suggests that immobilisation of specific glycans at carbon electrodes might offer new safe and sustainable routes for regulating colonisation of selected bacteria at bioanodes, ultimately influencing the composition of the catalytic biofilm community obtained at the electrode interface from a mixed inoculum.

Electrode materials were modified via electrografting of aryldiazonium bearing a *p*-mannoside functionality; covalent attachment was achieved via spontaneous reaction and via electrochemically assisted grafting using potential steps of different durations. We first discuss the effect of the different functionalisation protocols on wettability, roughness and electrochemical response of modified surfaces. Then we evaluate the performance of graphite rod electrodes to determine the effect of phenylmannoside adlayers on bioanode development, power output and overall electrochemical performance in an operational MFC.

2. Experimental methods

2.1. Materials

Glutaraldehyde solution 25% was purchased from VWR Chemicals. Sodium phosphate monobasic (ReagentPlus $\geq 99\%$), sodium phosphate dibasic (BioReagent $\geq 99\%$), sodium acetate (BioXtra $\geq 99\%$), potassium chloride (BioXtra $\geq 99\%$) and ammonium chloride (min. 99.5%) were all purchased from Sigma Aldrich. Potassium hexacyanoferrate(II) trihydrate (ANALAR) was purchased from BDH; potassium hexacyanoferrate(III) (ACS reagent $\geq 99\%$) was purchased from Fluka. 4-aminophenol- α -D-mannopyranose (Fig. 1) was synthesized following published protocols [39,40]. Glassy carbon (GC) disk electrodes were purchased from HTW (Sigradur, \varnothing 0.50 cm); indium tin oxide (ITO) coated glass (7 Ω per square) was purchased from Xin Yan Technology Ltd; graphite rods (GR) were purchased from Morgan Carbon (France). Fumasep FTAM-E anion exchange membrane PET-reinforced was purchased from Fumatech BWT.

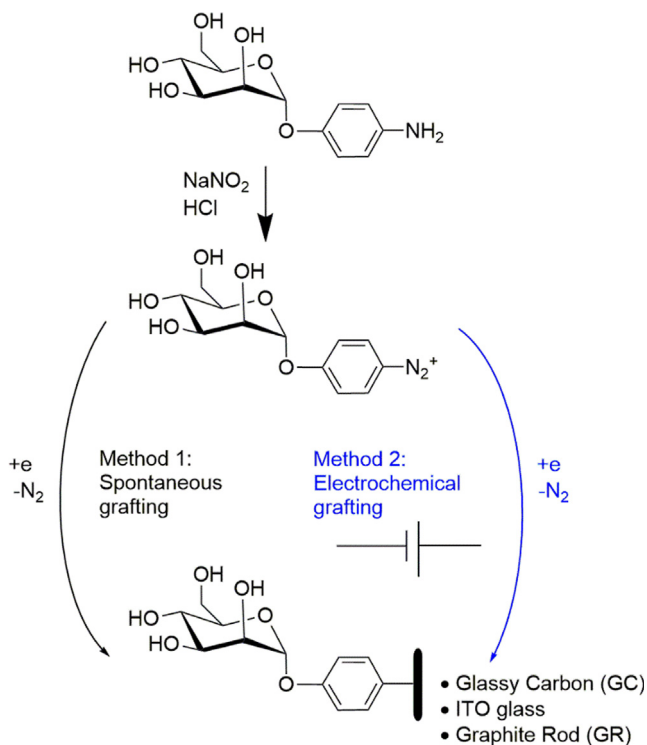


Fig. 1. Formation *in situ* of 4-aminophenol- α -D-mannopyranose diazonium cation and subsequent covalent attachment at surfaces via spontaneous (Method 1) and electrochemically assisted reduction (Method 2).

2.2. Substrate preparation and functionalization

Prior to surface modifications and electrochemical studies GC electrodes were polished with progressively finer grades of alumina slurry (Buehler) according to published protocols [48–50], whereas GR electrodes were polished with sand paper (1200 grit) and subsequently sonicated in deionised water, acetone and methanol (5 min in each solvent). Surface modifications were carried out in a degassed 1.0 mM solution of the aryldiazonium salt prepared *in situ* from its *p*-aminophenyl precursor (Fig. 1). Briefly, 10.0 mL of 10.0 mM NaNO₂ were added dropwise to a solution of 14 mg of 4-aminophenol- α -D-mannopyranose precursor in 40 mL of 1.8 mM HCl in an ice bath, yielding a 1.0 mM aqueous solution of the diazonium product. Two different grafting methods were explored, as in Fig. 1: spontaneous reaction with carbon surfaces (Method 1) and electrochemically assisted grafting via potential step (Method 2). In Method 1, substrates were immersed in the cation solution for 2 h at room temperature in the dark [42,51]. In Method 2, substrates were used as the working electrode in a 3-electrode cell (see Fig. 1) and a potential of -0.7 V vs SCE was applied for 35 s or 350 s [52]. After modification GC electrodes were rinsed as in previous work [41], while GR and ITO samples were rinsed in deionized water prior to further use. GC disks (\emptyset 0.50 cm) had an area defined by their geometry (0.196 cm²) while the area of GR and ITO electrodes was defined at 2.2 cm² and 0.91 cm², respectively, using a teflon tape to enable current and power density normalizations.

2.3. Characterization

Electrochemical characterization and potential step functionalizations were carried out using a potentiostat (Metrohm Autolab AUT50324) and a 3-electrode cell with a reference electrode, a graphite rod as counter electrode, and the substrate under study (GC, ITO or GR) as the working electrode. Water contact angle (WCA) measurements were performed using the sessile drop method (FTA1000). Atomic force microscopy (AFM, Asylum Research) was carried out using Au-coated cantilevers (obtained from NT-MDT Spectrum Instruments) in tapping mode. All errors on numerical values are calculated as standard deviations for $n = 3$, unless otherwise noted. Scanning electron microscopy (SEM) images were acquired on a Zeiss Ultra Plus field emission scanning electron microscope. Biofilm SEM imaging was performed following the protocol reported by Picot et al. [33]: briefly, the anodes were cut to lengths of approx. 0.5 cm using pliers; subsequently, the samples were collected and fixed overnight with a solution made of 0.1 M phosphate buffer and 2.5% vol. of glutaraldehyde; finally, they were washed with phosphate buffer and immersed in aqueous solutions containing progressively increasing ethanol concentrations (60, 70, 80, 90 and 100% ethanol), for 15 min in each solution. After this procedure the samples were critical point dried to replace the remaining water with CO₂ and they were Au-coated with a sputtering time of 20 s before SEM analysis.

2.4. Microbial fuel cell (MFC) studies

Double chamber MFC devices were fabricated from polycarbonate with ca. 85 mL capacity in each compartment. A circular membrane port \emptyset 1.8 cm connected the anodic and cathodic compartments which were sealed with independent covers, each equipped with 3 testing ports for electrode mounting and characterization. GR electrodes were fitted and suspended in the two compartments through rubber stoppers. The anodic solution consisted of 50/50 vol% wastewater (Beaurade Wastewater Treatment Plant, Rennes, France [53]) and phosphate buffer saline (PBS) solution consisting of 0.032 M Na₂HPO₄, 0.018 M NaH₂PO₄, 6.0 mM

NH₄Cl and 2.0 mM KCl [54]. Sodium acetate was added to the resulting mixture of PBS and wastewater, resulting in a final sodium acetate concentration of 0.012 M in the final solution. The cathodic solution consisted of 0.1 M K₃[Fe(CN)₆] in 0.032 M Na₂HPO₄ and 0.018 M NaH₂PO₄; the hexacyanoferrate (III) served as the electron acceptor and the 0.1 M concentration was confirmed to ensure a stable cathodic potential over the duration of MFC experiments [33]. After setup, the anode compartment was left under anaerobic conditions; MFCs were connected to 1000 Ω load and kept in a thermostated bath at 25.0 ± 0.1 °C over the duration of experiments. To ensure nutrient availability, sodium acetate (equivalent to an additional 0.012 M concentration) was added to the anodic compartment of all cells after 14 days of operation as discussed in the main text.

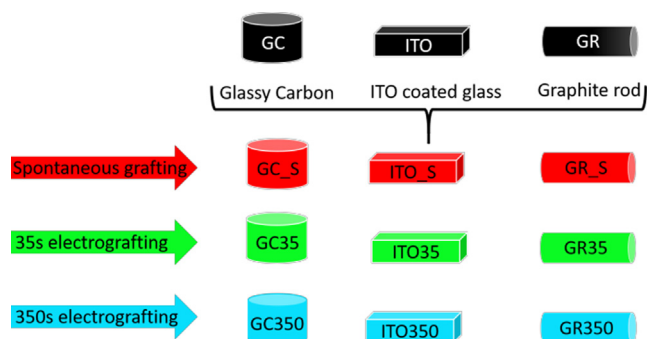
Power density curves and cell potentials were recorded over time to monitor MFC performance. Each MFC was connected to a decade resistance box (Elenco) and MFC output potentials were acquired with a multimeter (Keithley 2700) connected to a PC, as previously described [51,55–57]. Power density curves were obtained by first connecting each MFC to a 4 M Ω resistor for 2 h to acclimate the cells to the open circuit condition; then the resistance was progressively decreased in the range 10000–10 Ω at 30 min steps, while the output potential was recorded by the multimeter [55,56]. Cyclic voltammetry (CV) of MFC anodes was obtained in a 3-electrode configuration at 5 mV s⁻¹: the GR anode was used as working electrode, a saturated calomel reference electrode (SCE, IJ Cambria) was inserted in the anodic compartment through a testing port and the GR cathode was used as counter electrode. Two cycles were recorded; the second cycle of each measurement is shown in all cases.

3. Results and discussion

3.1. Mannoside immobilization via spontaneous and electrochemical grafting

Aryl-mannoside layers were immobilized on electrode surfaces using either spontaneous covalent attachment or electrochemically assisted grafting from aqueous solutions. The aryldiazonium salt derivative of 4-aminophenol- α -D-mannopyranose was prepared via a diazotization reaction as shown in Fig. 1; the covalent attachment was carried out *in situ* in the diazotization solution using a 1.0 mM concentration of the aminophenol precursor in all cases. The characterization of aryl-glycoside adlayers prepared via aryldiazonium cation reactions at carbon and at a variety of other substrates has been reported in detail in previous work from our group [39–43,58,59]. Briefly, a combination of microscopy and spectroscopic methods provides evidence that aryl-glycosides can be immobilized via either spontaneous or electrochemically assisted methods at carbon. Binding assays using fluorescently labeled lectins also demonstrate that grafted aryl-glycosides present at the surface can be specifically recognised by the corresponding lectins. Spontaneous reaction leads to the formation of homogeneous sub-nm adlayers (0.5–0.9 nm), while electrochemical grafting enables the formation of denser adlayers that remain however of average thickness <2 nm [58,59] on smooth substrates.

To investigate the effects of density and morphology of the aryl-mannoside adlayer on bioanodes, three grafting protocols were explored: spontaneous attachment (2 h) or -0.7 V vs SCE applied potential for 35 or 350 s. Three different substrates were used to characterise the resulting glycan adlayers, as illustrated in Scheme 1: glassy carbon (GC) and indium tin oxide (ITO) electrodes were used to probe the effects of grafting protocol on well characterized electrode substrates, whereas graphite rods (GR) were used for all microbial fuel cell experiments as discussed in later sections.



Scheme 1. Schematic illustrating the preparation of aryl-mannoside modified samples on glassy carbon (GC), indium tin oxide (ITO) and graphite rod (GR) substrates.

Fig. 2a shows cyclic voltammograms (CV) of mannoside-modified GC electrodes in 1.0 mM $K_4[Fe(CN)_6]$ solution in 0.5 M KCl obtained at 10 mV s^{-1} . All CVs display the characteristic reversible redox response of the $Fe(CN)_6^{3-/4-}$ couple. Spontaneous modification with aryl-mannoside groups results in a peak-to-peak potential difference (ΔE_p) of 67 mV which is close to the 59 mV separation expected for the one-electron Nernstian response of a reversible redox couple. The ΔE_p value was found to increase only marginally as a function of scan rate (see Supporting Information) thus indicating that spontaneous reaction of GC electrodes with aryldiazonium cations bearing mannoside groups results in electrodes with a quasi-reversible faradaic response towards $Fe(CN)_6^{3-/4-}$, in agreement with previous findings obtained using a lactoside analog of the precursor in Fig. 1 [59].

Potential steps of 35 and 350 s in the 1.0 mM diazotiation solution resulted in electrografted GC electrodes, indicated as GC35 and GC350, respectively. These surfaces were found to display greater passivating properties than those obtained via spontaneous reaction. This is evidenced in Fig. 2a by ΔE_p values larger than 100 mV for both GC35 and GC350 that increase rapidly with scan rate (see Supporting Information), and by a significant depression in the current peaks clearly observed for GC350. This is diagnostic of an additional impedance to charge transfer characteristic of the presence of a passive film [49,60]. The total integrated cathodic charge densities associated with the generation of aryl radicals during the potential step experiments were 26 ± 5 and $98 \pm 30 \text{ C m}^{-2}$ for GC35 and GC350, respectively (see Supporting Information). These values are well in excess of the total charge density required for electrografting an aryldiazonium monolayer (ca. 10^{-6} – $10^{-5} \text{ mol m}^{-2}$ equivalent to 0.1 – 1.0 C m^{-2}) at a topographically smooth surface [39,41]. Therefore, CV results indicate that GC35 and GC350 samples are likely to display denser aryl-mannoside adlayers than those obtained spontaneously, in agreement with recent reports using aryl-lactoside precursors [59]. The trends in CV waveforms also suggest that denser films are obtained after electrografting for the longer potential step, as longer grafting times result in enhanced current depression and increase of ΔE_p values of $Fe(CN)_6^{3-/4-}$ peaks.

Fig. 2b–d show AFM images of substrates modified spontaneously, and via potential steps of 35 and 350 s, respectively; experiments were carried out in this case using ITO substrates because of their smoother topography (rms roughness $3.01 \pm 0.03 \text{ nm}$; see Supporting Information) relative to that of polished GC [48] or GR (see Supporting Information). AFM imaging shows that the functionalization method significantly affects the morphology

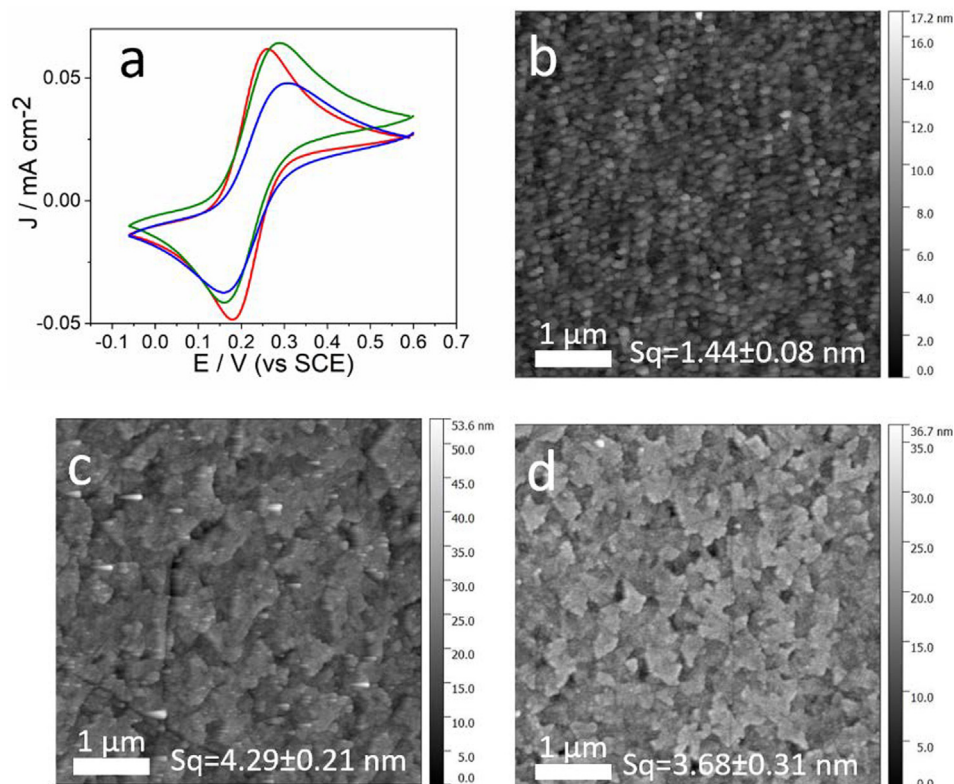


Fig. 2. (a) Cyclic voltammograms in 1.0 mM $K_4[Fe(CN)_6]$ in 0.5 M KCl at 10 mV s^{-1} of mannoside-modified GC electrodes prepared via spontaneous reaction (GC_S, red), and via electrografting for 35 s (GC35, green) and 350 s (GC350, blue). AFM images of ITO substrates modified with aryl-mannoside adlayers via (b) spontaneous reactions, (c) electrografting for 35 s and (d) electrografting for 350 s; the average values of rms roughness (S_q) are shown for each of the respective images. (For interpretation of the references to colour in this figure legend, the reader is referred to the web version of this article.)

of the aryl-mannoside adlayer. The spontaneously modified surface displays an rms roughness of 1.44 ± 0.08 nm, a value lower than that of the bare substrate (see Supporting Information). These results indicate that spontaneous grafting yields conformal saccharide layers that are smoother than the original substrate, in agreement with previous findings using nitrobenzene diazonium salts [51]. Electrografting for 35 and 350 s results in a significant increase in the rms roughness to 4.3 ± 0.2 nm and 3.7 ± 0.3 nm, respectively, that is indicative of the presence of disordered glycan adlayers [61–63].

Microbial fuel cells were assembled using graphite rods (GR) as electrodes in both the anodic and cathodic compartments, as these carbon materials are among the most popular for MFC anodes due to their low resistivity, widespread availability and low cost [64]. The properties of aryl-mannoside adlayers were therefore also studied on these carbon substrates. Fig. 3a shows a CV recorded at 10 mV s^{-1} in $1.0 \text{ mM K}_4[\text{Fe}(\text{CN})_6]$ solution in 0.5 M KCl of a bare GR and of mannoside-modified GR via 35 s (GR35) or 350 s (GR350) electrografting at -0.7 V . After electrografting, negligible passivation to $\text{Fe}(\text{CN})_6^{3/-4}$ charge transfer is observed at GR electrodes, as evidenced by the presence of quasi-reversible peaks with similar ΔE_p compared to that on bare GR. This indicates that the adlayers formed on GR substrates are likely to be sparse and defective, despite application of identical electrografting protocols as for GC. The total integrated cathodic charge densities associated with the generation of aryl radicals during the potential steps were 64 ± 14 and $447 \pm 124 \text{ C m}^{-2}$ for GR35 and GR350, respectively (see also Supporting Information). Despite the difference in total cathodic charge density, the two electrografted GR electrodes result in very similar electrochemical passivation. Interestingly,

the values of integrated cathodic charge density are significantly larger than those observed in the case of GC, thus indicating that the near reversible response at GR cannot be attributed to a lower concentration of reactive radical species during grafting relative to GC. Therefore, it appears more likely that differences arise instead from a larger specific surface area available at GR vs GC surfaces, a hypothesis supported by roughness determinations of polished GR (see Supporting Information) and significantly larger current densities than for GC electrodes.

Aryldiazonium modification with glycan derivatives has been previously shown to result in a significant increase in surface free energy and hydrophilic character [58]. Given that wettability is typically highlighted as a factor controlling the activity of bioanodes [34,65], we examined the effect of covalent attachment of mannoside groups at the GR surface using water contact angle (WCA) measurements. WCA results are shown in Fig. 3b and in Supporting Information. The polished GR surface yields a value of $94^\circ \pm 5^\circ$, close to that reported for pyrocarbon and pyrolyzed resist carbon films [66] but lower relative to typical carbon materials used in MFC studies, such as carbon papers [67,68], carbon cloths [69,70] and felts [71] (WCA greater than 100°). Grafting of aryl-mannosides results in a decrease in water contact angle to $87^\circ \pm 3^\circ$, $67^\circ \pm 6^\circ$ and $70^\circ \pm 9^\circ$ for spontaneously grafted, 35 s electrografted and 350 s electrografted adlayers, respectively. This shows that spontaneous grafting results in a slight increase in hydrophilic character whereas a very significant increase in hydrophilic character is observed at the GR surface after electrografting during 35 or 350 s. This supports the conclusion that electrografting yields denser adlayers compared to spontaneous grafting despite the level of electrochemical passivation being similar on GR after both of these treatments (spontaneous or electrografting modification, see Fig. 3a).

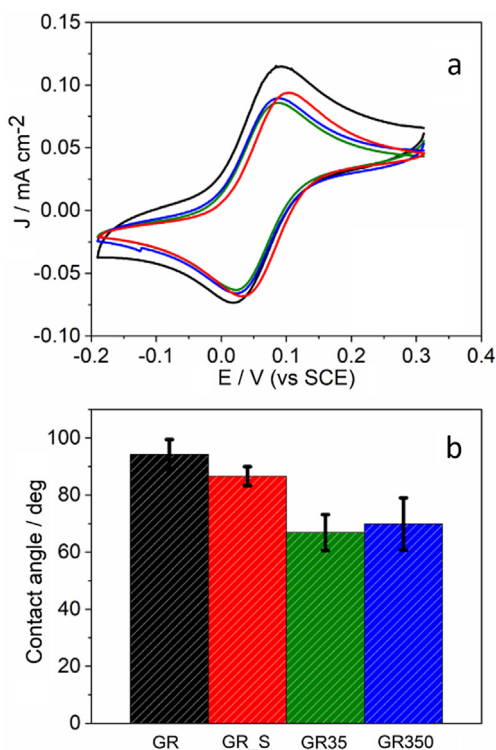


Fig. 3. (a) Cyclic voltammograms in $1.0 \text{ mM K}_4[\text{Fe}(\text{CN})_6]$ in 0.5 M KCl obtained at 10 mV s^{-1} of polished GR (black), spontaneously grafted GR (GR_S red), and mannoside-modified GR via electrografting for 35 s (GR35, green) and 350 s (GR350, blue). (b) Water contact angle values obtained for polished bare GR surfaces, and for GR surfaces modified with aryl-mannoside groups via spontaneous reactions and electrografting. (For interpretation of the references to colour in this figure legend, the reader is referred to the web version of this article.)

3.2. Microbial fuel cell studies of glycan modified anodes

The performance of GR electrodes as bioanodes was evaluated in double-chamber MFC devices; all cells possessed identical geometry and are shown in Supporting Information. GR electrodes that had undergone one of the three treatments were tested: conventional polishing (GR), spontaneous grafting with aryl-mannosides (GR_S), or electrografting with aryl-mannosides for 350 s (GR350). During the initial start-up, the cells were all inoculated with 50/50 vol% wastewater/PBS containing 0.012 M sodium acetate, following previous protocols.[54] All cells were kept in a thermostated bath (25°C) over the duration of experiments with a 1000Ω load connected to the leads when not under testing.

The potential of the MFC was acquired over time by connecting the leads to a 1000Ω resistance [72–74]. Fig. 4 shows the evolution of the potential over time; after 10 days all cells equipped with aryl-mannoside modified GR anodes develop significantly higher potentials than cells equipped with bare anodes, thus indicating faster start-up time of the electroactive anodic biofilm. This was further confirmed via power density curves obtained by varying the cell load, shown in Fig. 5a and b at day 12 and 17, respectively; characteristic values of power density are also summarized in Table 1. The power density curves show that MFCs prepared with aryl-mannoside adlayers at the anodes deliver a maximum power density at day 12 that is 20–80 times larger than that of MFCs with bare GR. This difference can be confirmed to result from a faster rate of biofilm development on aryl-mannoside adlayers and not from a failure of colonization, given that all cells eventually converge to similar maximum power outputs at day 17.

The activity of the anodic biofilms was further investigated via CV using the anode as the working electrode in a three-electrode configuration. Fig. 6a shows examples of CVs obtained for a bare GR, GR_S and GR350 anodes at 11 days of operation; the CVs of

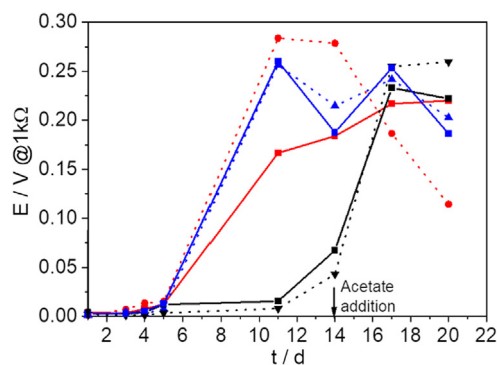


Fig. 4. Potential of all MFCs tested as a function of time from inoculation: GR#1 (continuous black), GR#2 (dashed black), GR_S#1 (continuous red), GR_S#2 (dashed red), GR350#1 (continuous blue), GR350#2 (dashed blue). Potentials were measured under a 1 k Ω load. Arrows indicate times at which sodium acetate was added to the anodic compartment. (For interpretation of the references to colour in this figure legend, the reader is referred to the web version of this article.)

all anodes tested are reported in [Supporting Information](#). The CVs of anodes modified with aryl-mannoside groups show the characteristic waveform of the biocatalyzed oxidation of acetate at a mature biofilm, with an onset potential at ca. -0.45 V vs SCE [30,33,75]. The anodes that consist of bare GR show lower currents and an absence of biocatalytic activity suggests that the bioanode is still under development [76]. The small redox peaks around -0.1 V to -0.3 V vs SCE are tentatively assigned to electroactive pioneer species not fully capable of catalytic activity towards acetate oxidation [76–78]. After 14 days of operation, a drop was observed in the current densities of CVs for almost all anodes (Fig. 6b); small redox peaks due to cross-contamination from the catholyte were also observed at ca. 0.1 V. The anodic compartment was therefore replenished with sodium acetate (addition of 0.012 M equivalent) to continue biofilm growth. CVs in Fig. 6c obtained at day 18 show a clear onset for acetate oxidation at ca. -0.45 V vs SCE and high anodic current density for bare GR anodes, thus confirming that eventually all GR electrodes develop biocatalytic activity. This is also evident from maximum power densities reported in Table 1, which indicate that after 18 days all bioanodes display comparable performance. Biofilm morphology obtained at day 18 over the different bioanodes was then evaluated with SEM. Fig. 7 shows SEM images of three representative samples: GR#1, GR_350#1, and GR_S#1. The biofilms are homogeneous over all three considered electrodes; a mature biofilm is observed over the three different surfaces, in agreement with the comparable

Table 1
Evolution of power density values of MFCs studied.

Anode	Maximum power density (mW m^{-2})	
	day 12	day 17
GRbare #1	12	359
GRbare #2	5	353
GR_S #1	242	320
GR_S #2	397	330
GR350 #1	258	325
GR350 #2	347	334

polarization performances obtained at day 17 (Fig. 5b, Table 1). From the SEM analysis of the three samples it is also possible to conclude that the grafted phenyl-mannoside layer is compatible with electroactive bacteria due to the presence of similar biofilm over the surface of the considered electrodes.

4. Discussion

Graphite rod electrodes were modified with phenyl-mannoside adlayers using two different protocols and were subsequently used as MFC anodes to test the effect of the glycan functional layer on MFC performance. Modification with mannoside groups was found to offer a facile method for regulating the wettability of anode materials. Despite observing differences in the WCA at graphite rods between spontaneously and electrochemically modified electrodes, no changes in the impedance to charge transfer were observed when using passivation tests with the ferri/ferrocyanide redox couple. This indicates that aryldiazonium reactions can be used to regulate wettability of graphite anodes without a trade-off in electrochemical response.

The presence of phenyl-mannosides is clearly beneficial for accelerating cell start-up. This is evident from the rapid rise of cell potential under charge transfer conditions (1 k Ω load) in the case of mannoside-modified anodes after only 5 days from inoculation with wastewater, independently of modification protocol. By contrast, bare graphite rods do not show significant cell potentials until day 14. Further evidence of faster start-up emerges from power density curves which confirm that bioanode evolution is accelerated for modified graphite electrodes: the maximum power density on functionalized bioanodes was in fact found to be 20–80 times larger for mannoside-modified materials relative to bare graphite rods at day 11. These differences cannot be ascribed to failed colonization of control anodes, as eventually all MFCs converge to similar power density outputs at day 17 and to similar biofilm den-

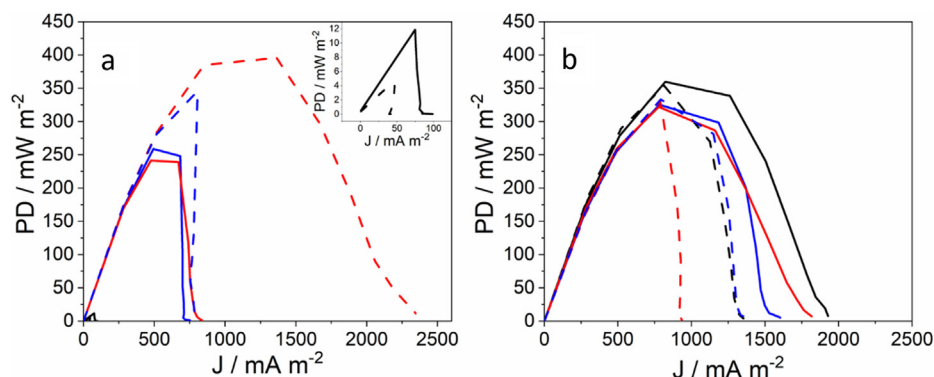


Fig. 5. Power density curves of MFCs equipped with GR grafted electrodes as anodes and compared with bare GR: GR#1 and GR#2 (continuous and dashed black curves, respectively), GR350#1 and GR350#2 (continuous and dashed blue curves, respectively), GR_S#1 and GR_S#2 (continuous and dashed red curves, respectively). Curves were obtained after 12 (a) and 17 (b) days of operation; the inset shows expanded version of the data for GR#1 and GR#2. (For interpretation of the references to colour in this figure legend, the reader is referred to the web version of this article.)

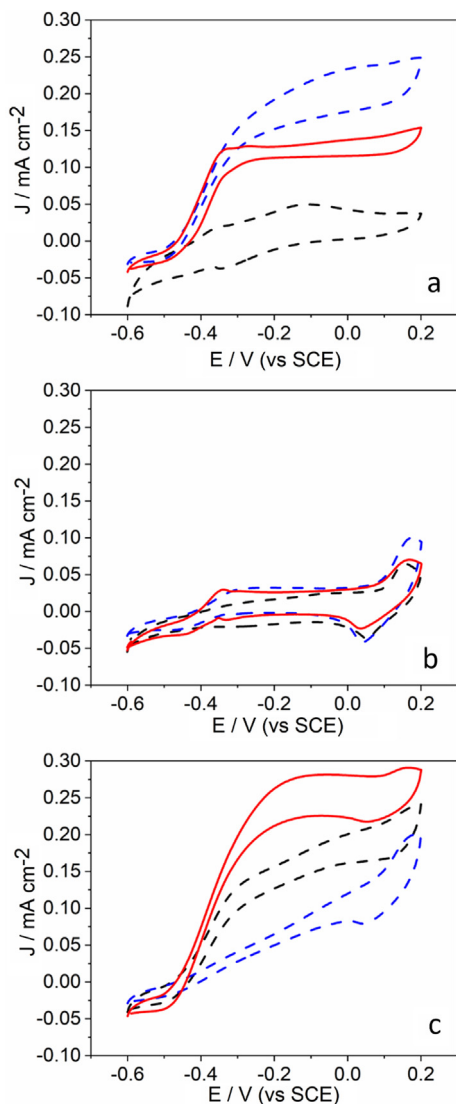


Fig. 6. In situ CVs of graphite anodes in the anodic compartment obtained at 5 mV s^{-1} after day 11 (a), day 14 (b) and day 18 (c): GR#2 (dashed black), GR350#2 (dashed blue) and GR_S#1 (continuous red). (For interpretation of the references to colour in this figure legend, the reader is referred to the web version of this article.)

sities as confirmed via SEM imaging of bioanodes. These results therefore indicate that modification with glycans can be leveraged to enhance the rate of biofilm colonization from a mixed inoculum without any adverse effects on final MFC outputs.

Cyclic voltammetry of bioanodes shows that the power density increases at day 11 are due to the presence of a mature biofilm. The bio-catalytic wave observed at -0.45 V vs. SCE is diagnostic of electrode coupling to outer membrane cytochromes [33,79,80]. This biocatalytic wave is absent at bare graphite electrodes but eventually becomes evident at day 18, thus indicating that biofilm maturation is slower on the unmodified electrode surfaces.

It is interesting to note that differences in aryldiazonium grafting methods do not translate into significant differences in the maximum power densities observed for the MFCs, i.e. the best performances with spontaneously and electrochemically grafted mannoses are 397 and 347 mW m^{-2} , respectively. This is in contrast with previous observations on the effect of aryldiazonium electrografting charge reported by Picot et al. [33] using a range of chemical functionalities and could be explained by the lower temperature used in that work and with the thinner coatings obtained in this work with the saccharide functionalized aryldiazonium [33,41,58]. In the case of the MFC anodes in our work, we were not able to observe significant differences in passivation between spontaneously and electrochemically modified electrodes despite electrografting typically resulting in much denser films. The lack of passivation is likely due to the significant specific surface area and roughness of polished graphite rods (see Supporting Information) which results in a high density of sites available for grafting. However, we observed noticeable differences in the replicability of the performance at day 11 between the two grafting methods: at day 11, the two electrografted bioanodes display a relative variability of only 25% in maximum power density, whereas spontaneously grafted anodes yield a 40% variability in peak values. This suggests that spontaneous grafting is more likely to result in performances intermediate to those of bare and electrografted graphite anodes. We propose that the higher glycan densities achievable with electrografted methods are beneficial in presenting homogeneous mannose adlayers at these highly rough electrode surfaces, in agreement with trends of increasing wettability observed via WCA measurements.

Finally, it is interesting to consider the origin of faster start-up times observed for mannose-modified graphite anodes. Bioanode development has been shown to be affected by changes in surface charge, morphology/porosity and hydrophilicity in the anode car-

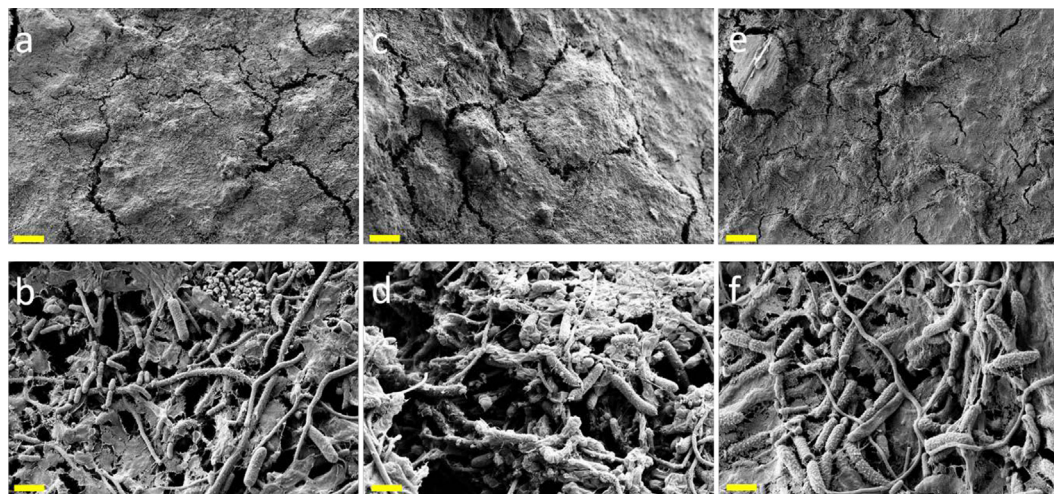


Fig. 7. Scanning electron micrographs of GR#1 (a, b), GR_350#1 (c, d), and GR_S#1 (e, f) obtained after 18 days of operation. Scalebars equivalent to $20 \mu\text{m}$ (a, c and e) and $1 \mu\text{m}$ (b, d and f).

bon material resulting from surface modifications. Prior work from our group demonstrated that, unlike oxidative treatments [81], glycoside immobilization via aryldiazonium chemistry does not result in changes in the surface electrostatic charge [58]. Therefore, attractive/repulsive interactions are not expected to be significantly different for biofilm/mannoside-electrode vs. biofilm/unmodified graphite interfaces. Also, the increase in surface roughness resulting from aryldiazonium electrografting is negligible compared to the original roughness of polished graphite rod surfaces; therefore, changes in electrode morphology can be excluded as a factor in accelerating bioanode development. Mannoside-immobilization introduces polyhydroxylated moieties that increase the hydrophilicity, which has been proposed to correlate with faster start up times [67,82]. The polished graphite rods display a WCA value that is slightly above the limit of the conventional hydrophobic/hydrophilic threshold (90°) [83], and are hydrophilic relative to the most common MFC anode materials. Spontaneous modification with mannosides results in a minor reduction in water contact angle (from 94° to 87°), while development of a mature biofilm is substantially accelerated. Although it is not possible to completely exclude that the increase in hydrophilic character contributes to faster biofilm development, the change in WCA appears small ($<10^\circ$) compared to those reported in the MFC literature to affect bioanode performance. Therefore, it appears likely that the functional role of glycans in biofilm development might also contribute to the observed enhancements. Cell agglutination and surface adhesion can be favoured via lectin-carbohydrate binding interactions; these interactions are known to play a role in bacterial adhesion, biofilm formation and surface colonization [84]. It is known that bacteria such as *E. Coli* show specific binding to glycosides, in the case of mannosides it is mediated by the FimH adhesin [63,64]. Therefore it appears likely that these bio-functional phenyl-mannoside adlayers might contribute to the regulation of bioanode development through signaling pathways that directly facilitate adhesion of exoelectrogenous species, or that condition the surface with bacterial communities that promote adhesion of bioelectroactive species at a later stage. Further studies into the role of specific, surface-bound glycans in modulating bioanode development are ongoing in our labs.

5. Conclusions

Surface functionalization of graphite anode materials with mannoside adlayers was found to result in accelerated start-up of microbial fuel cells. Modified graphite materials were found to develop a catalytic biofilm faster than control bare graphite surfaces. Modified bioanodes yielded the characteristic catalytic waves of acetate oxidation in cyclic voltammograms at an estimated 40% faster rate than bare anodes. Similarly, the power density performances developed faster and reached their limiting values earlier under working operative conditions at glycan-modified anodes.

The effects of surface modification protocol and final glycan density were also investigated. Cell anodes were obtained by functionalizing MFC anodes with aryl-mannoside adlayers using two different grafting strategies: spontaneous and electrochemically driven grafting. Even if both of these strategies result in high power outputs we observed noticeable differences in the replicability of the performance at day 12 between the two grafting methods: the two electrografted bioanodes display lower variability in power density peaks than the spontaneously grafted anodes. We propose that the higher glycan densities achieved via electrografting are beneficial in presenting homogeneous mannoside adlayers at these highly rough electrode surfaces, in agreement with trends of increasing wettability observed via WCA measurements.

Our results demonstrate that functionalization of carbon electrodes with glycan adlayers via aryldiazonium reactions offers a method for enhancing the development of electroactive microbial biofilms. The enhancement in the MFC start-up times is likely to arise from a combination of increased wettability and binding affinity towards bacterial receptors in the biofilm. Cell agglutination and surface adhesion might be mediated via lectin-carbohydrate interactions which are known to play a role in cell adhesion, biofilm formation and surface colonization. Further enhancements in MFC performance might be possible through immobilization of biomimetic oligosaccharide moieties that can elicit specific cell behaviour at the anode interface.

Declaration of Competing Interest

The authors declare that they have no known competing financial interests or personal relationships that could have appeared to influence the work reported in this paper.

Acknowledgements

This project has received funding from the European Union's Horizon 2020 research and innovation programme under the Marie Skłodowska-Curie grant agreement No. 799175 (HiBriCarbon). The results of this publication reflect only the authors' view and the Commission is not responsible for any use that may be made of the information it contains. This publication has also emanated from research conducted with the financial support of Science Foundation Ireland under Grant No. 13/CDA/2213. The authors also thank the France-Ireland PHC ULYSSES programme for support, project 36028UB. JAB acknowledges support from the Irish Research Council under Grant No. GOIPG/2014/399. The authors are also grateful to Dr. Sciarria from University of Milan for valuable suggestions. The authors are also grateful to Dr. M. Canavan of the Advanced Microscopy Laboratory for assistance with SEM imaging.

Appendix A. Supplementary material

Supplementary data to this article can be found online at <https://doi.org/10.1016/j.bioelechem.2020.107621>.

References

- [1] M.C. Potter, A.D. Waller, Electrical effects accompanying the decomposition of organic compounds, *Proc. R. Soc. London, B* 84 (1911) 260–276.
- [2] M. Thomas, M.C. Potter, *Nature* 161 (1948) 673–674.
- [3] B.E. Logan, *Microbial Fuel Cells*, Wiley, Hoboken, New Jersey, 2008.
- [4] A.J. Slate, K.A. Whitehead, D.A.C. Brownson, C.E. Banks, *Microbial fuel cells: An overview of current technology*, *Renew. Sustain. Energy Rev.* 101 (2019) 60–81.
- [5] J.L. Liu, D.A. Lowy, R.G. Baumann, L.M. Tender, Influence of anode pretreatment on its microbial colonization, *J. Appl. Microbiol.* 102 (2007) 177–183.
- [6] P. Zhang, J. Liu, Y. Qu, D. Li, W. He, Y. Feng, Nanomaterials for facilitating microbial extracellular electron transfer: Recent progress and challenges, *Bioelectrochemistry* 123 (2018) 190–200.
- [7] G. Pankratova, L. Gorton, Electrochemical communication between living cells and conductive surfaces, *Curr. Opin. Electrochem.* 5 (2017) 193–202.
- [8] C.-E. Zhao, P. Gai, R. Song, Y. Chen, J. Zhang, J.-J. Zhu, Nanostructured material-based biofuel cells: recent advances and future prospects, *Chem. Soc. Rev.* 46 (2017) 1545–1564.
- [9] C. Santoro, C. Arbizzani, B. Erable, I. Ieropoulos, *Microbial fuel cells: From fundamentals to applications. A review*, *J. Power Sources* 356 (2017) 225–244.
- [10] R.A. Rozendal, H.V. Hamelers, K. Rabaey, J. Keller, C.J. Buisman, Towards practical implementation of bioelectrochemical wastewater treatment, *Trends Biotechnol.* 26 (2008) 450–459.
- [11] F. Yu, C. Wang, J. Ma, Applications of graphene-modified electrodes in microbial fuel cells, *Materials (Basel)* 9 (2016) 807.
- [12] P. Champigneux, C. Renault-Sentenac, D. Bourrier, C. Rossi, M.-L. Delia, A. Bergel, Effect of surface nano/micro-structuring on the early formation of microbial anodes with *Geobacter sulfurreducens*: Experimental and theoretical approaches, *Bioelectrochemistry* 121 (2018) 191–200.

- [13] P. Bakonyi, L. Koók, T. Rózsenszki, G. Tóth, K. Bélafi-Bakó, N. Nemestóthy, Development and application of supported ionic liquid membranes in microbial fuel cell technology: a concise overview, *Membranes* 10 (2020) 16.
- [14] X. Liu, W. Wu, Z. Gu, Poly (3,4-ethylenedioxythiophene) promotes direct electron transfer at the interface between *Shewanella loihica* and the anode in a microbial fuel cell, *J. Power Sources* 277 (2015) 110–115.
- [15] B. Logan, S. Cheng, V. Watson, G. Estadt, Graphite fiber brush anodes for increased power production in air-cathode microbial fuel cells, *Environ. Sci. Technol.* 41 (2007) 3341–3346.
- [16] S.K. Chaudhuri, D.R. Lovley, Electricity generation by direct oxidation of glucose in mediatorless microbial fuel cells, *Nat. Biotechnol.* 21 (2003) 1229–1232.
- [17] M. Di Lorenzo, K. Scott, T.P. Curtis, I.M. Head, Effect of increasing anode surface area on the performance of a single chamber microbial fuel cell, *Chem. Eng. J. (Lausanne)* 156 (2010) 40–48.
- [18] X. Chen, D. Cui, X. Wang, X. Wang, W. Li, Porous carbon with defined pore size as anode of microbial fuel cell, *Biosens. Bioelectron.* 69 (2015) 135–141.
- [19] W. Wu, H. Niu, D. Yang, S. Wang, N. Jiang, J. Wang, J. Lin, C. Hu, Polyaniline/carbon nanotubes composite modified anode via graft polymerization and self-assembling for microbial fuel cells, *Polymers* 10 (2018) 759.
- [20] B. Lai, X. Tang, H. Li, Z. Du, X. Liu, Q. Zhang, Power production enhancement with a polyaniline modified anode in microbial fuel cells, *Biosens. Bioelectron.* 28 (2011) 373–377.
- [21] Y.B. Fu, Z.H. Liu, G. Su, X.R. Zai, M. Ying, J. Yu, Modified carbon anode by MWCNTs/PANI used in marine sediment microbial fuel cell and its electrochemical performance, *Fuel Cells* 16 (2016) 377–383.
- [22] N. Zhu, X. Chen, T. Zhang, P. Wu, P. Li, J. Wu, Improved performance of membrane free single-chamber air-cathode microbial fuel cells with nitric acid and ethylenediamine surface modified activated carbon fiber felt anodes, *Bioresour. Technol.* 102 (2011) 422–426.
- [23] M. Zhou, M. Chi, H. Wang, T. Jin, Anode modification by electrochemical oxidation: A new practical method to improve the performance of microbial fuel cells, *Biochem. Eng. J.* 60 (2012) 151–155.
- [24] X. Tang, K. Guo, H. Li, Z. Du, J. Tian, Electrochemical treatment of graphite to enhance electron transfer from bacteria to electrodes, *Bioresour. Technol.* 102 (2011) 3558–3560.
- [25] J. Wei, P. Liang, X. Huang, Recent progress in electrodes for microbial fuel cells, *Bioresour. Technol.* 102 (2011) 9335–9344.
- [26] B. Li, J. Zhou, X. Zhou, X. Wang, B. Li, C. Santoro, M. Grattieri, S. Babanova, K. Artyushkova, P. Atanassov, A.J. Schuler, Surface modification of microbial fuel cells anodes: approaches to practical design, *Electrochim. Acta* 134 (2014) 116–126.
- [27] B. Cercado-Quezada, M.-L. Delia, A. Bergel, Electrochemical micro-structuring of graphite felt electrodes for accelerated formation of electroactive biofilms on microbial anodes, *Electrochem. Commun.* 13 (2011) 440–443.
- [28] S. Cheng, B.E. Logan, Ammonia treatment of carbon cloth anodes to enhance power generation of microbial fuel cells, *Electrochem. Commun.* 9 (2007) 492–496.
- [29] G.P. Moss, P.A.S. Smith, D. Tavernier, Glossary of class names of organic compounds and reactivity intermediates based on structure (IUPAC Recommendations 1995), *Pure Appl. Chem.* 67 (1995) 1307.
- [30] H. Smida, E. Lebègue, J.-F. Bergamini, F. Barrière, C. Lagrost, Reductive electrografting of in situ produced diazopyridinium cations: Tailoring the interface between carbon electrodes and electroactive bacterial films, *Bioelectrochemistry* 120 (2018) 157–165.
- [31] H. Smida, E. Lebègue, M. Cortes, J.-F. Bergamini, F. Barrière, C. Lagrost, Corrigendum to “Reductive electrografting of in situ produced diazopyridinium cations: Tailoring the interface between carbon electrodes and electroactive bacterial films” [Bioelectrochem. 120 (2018) 157–165], *Bioelectrochemistry*, 125 (2019) 70.
- [32] L. Lapinonnière, M. Picot, C. Poriol, F. Barrière, Phenylboronic acid modified anodes promote faster biofilm adhesion and increase microbial fuel cell performances, *Electroanalysis* 25 (2013) 601–605.
- [33] M. Picot, L. Lapinonnière, M. Rothballer, F. Barrière, Graphite anode surface modification with controlled reduction of specific aryl diazonium salts for improved microbial fuel cells power output, *Biosens. Bioelectron.* 28 (2011) 181–188.
- [34] K. Guo, S. Freguia, P.G. Dennis, X. Chen, B.C. Donose, J. Keller, J.J. Gooding, K. Rabaey, Effects of surface charge and hydrophobicity on anodic biofilm formation, community composition, and current generation in bioelectrochemical systems, *Environ. Sci. Technol.* 47 (2013) 7563–7570.
- [35] K. Guo, A. PrévotEAU, S.A. Patil, K. Rabaey, Engineering electrodes for microbial electrocatalysis, *Curr. Opin. Biotechnol.* 33 (2015) 149–156.
- [36] T. Saito, M. Mehanna, X. Wang, R.D. Cusick, Y. Feng, M.A. Hickner, B.E. Logan, Effect of nitrogen addition on the performance of microbial fuel cell anodes, *Bioresour. Technol.* 102 (2011) 395–398.
- [37] A. Kumar, P.Ó. Conghaile, K. Katuri, P. Lens, D. Leech, Arylamine functionalization of carbon anodes for improved microbial electrocatalysis, *RSC Adv.* 3 (2013) 18759–18761.
- [38] S. Rusli, M.H. Abu Bakar, S. Rani, K.S. Loh, M. Mastar, Aryl Diazonium Modification for Improved Graphite Fiber Brush in Microbial Fuel Cell, *Sains Malaysiana* 47 (2018) 3017–3023.
- [39] D.R. Jayasundara, T. Duff, M.D. Angione, J. Bourke, D.M. Murphy, E.M. Scanlan, P.E. Colavita, Carbohydrate coatings via aryldiazonium chemistry for surface biomimicry, *Chem. Mater.* 25 (2013) 4122–4128.
- [40] L. Esteban-Tejeda, T. Duff, G. Ciapetti, M. Daniela Angione, A. Myles, J.M. Vasconcelos, E.M. Scanlan, P.E. Colavita, Stable hydrophilic poly (dimethylsiloxane) via glycan surface functionalization, *Polymer* 106 (2016) 1–7.
- [41] A. Myles, J.A. Behan, B. Twamley, P.E. Colavita, E.M. Scanlan, Spontaneous aryldiazonium grafting for the preparation of functional cyclodextrin-modified materials, *ACS Appl. Bio Mater.* 1 (2018) 825–832.
- [42] A. Myles, D. Haberlin, L. Esteban-Tejeda, M.D. Angione, M.P. Browne, M.K. Hoque, T.K. Doyle, E.M. Scanlan, P.E. Colavita, Bioinspired aryldiazonium carbohydrate coatings: reduced adhesion of foulants at polymer and stainless steel surfaces in a marine environment, *ACS Sus. Chem. Eng.* 6 (2017) 1141–1151.
- [43] M.D. Angione, T. Duff, A.P. Bell, S.N. Stamatina, C. Fay, D. Diamond, E.M. Scanlan, P.E. Colavita, Enhanced antifouling properties of carbohydrate coated poly (ether sulfone) membranes, *ACS Appl. Mater. Interfaces* 7 (2015) 17238–17246.
- [44] F. Zen, V.D. Karanikolas, J.A. Behan, J. Andersson, G. Ciapetti, A.L. Bradley, P.E. Colavita, Nanoplasmonic sensing at the carbon-bio interface: study of protein adsorption at graphitic and hydrogenated carbon surfaces, *Langmuir* 33 (2017) 4198–4206.
- [45] P. Klemm, M.A. Schembri, Bacterial adhesins: function and structure, *Int. J. Med. Microbiol.* 290 (2000) 27–35.
- [46] K.A. Kline, S. Fälker, S. Dahlberg, S. Normark, B. Henriques-Normark, Bacterial adhesins in host-microbe interactions, *Cell Host Microbe* 5 (2009) 580–592.
- [47] N. Sharon, Carbohydrates as future anti-adhesion drugs for infectious diseases, *Biochim. Biophys. Acta, Gen. Subj.* 1760 (2006) 527–537.
- [48] J.A. Behan, A. Iannaci, C. Dominguez, S.N. Stamatina, M.K. Hoque, J.M. Vasconcelos, T. Perova, P.E. Colavita, Electrocatalysis of N-doped carbons in the oxygen reduction reaction as a function of pH: N-sites and scaffold effects, *Carbon* 148 (2019) 224–230.
- [49] J.A. Behan, S.N. Stamatina, M.K. Hoque, G. Ciapetti, F. Zen, L. Esteban-Tejeda, P.E. Colavita, Combined optoelectronic and electrochemical study of nitrogenated carbon electrodes, *J. Phys. Chem. C* 121 (2017) 6596–6604.
- [50] J.A. Behan, M.K. Hoque, S.N. Stamatina, T.S. Perova, L. Vilella-Arribas, M. García-Melchor, P.E. Colavita, Experimental and computational study of dopamine as an electrochemical probe of the surface nanostructure of graphitized N-doped carbon, *J. Phys. Chem. C* 122 (2018) 20763–20773.
- [51] D.R. Jayasundara, R.J. Cullen, P.E. Colavita, In situ and real time characterization of spontaneous grafting of aryldiazonium salts at carbon surfaces, *Chem. Mater.* 25 (2013) 1144–1152.
- [52] C. Combellas, F. Kanoufi, J. Pinson, F.I. Podvorica, Sterically hindered diazonium salts for the grafting of a monolayer on metals, *J. Am. Chem. Soc.* 130 (2008) 8576–8577.
- [53] H. Smida, T. Flinois, E. Lebègue, C. Lagrost, F. Barrière, Microbial Fuel Cells—Wastewater Utilization, in: K. Wandelt (Ed.), *Encyclopedia of Interfacial Chemistry*, Elsevier, Oxford, 2018, pp. 328–336.
- [54] F. Zhang, X. Xia, Y. Luo, D. Sun, D.F. Call, B.E. Logan, Improving startup performance with carbon mesh anodes in separator electrode assembly microbial fuel cells, *Bioresour. Technol.* 133 (2013) 74–81.
- [55] B.E. Logan, B. Hamelers, R. Rozendal, U. Schröder, J. Keller, S. Freguia, P. Aelterman, W. Verstraete, K. Rabaey, Microbial fuel cells: methodology and technology, *Environ. Sci. Technol.* 40 (2006) 5181–5192.
- [56] T.P. Sciarria, A. Tenca, A. D’Epifanio, B. Mecheri, G. Merlino, M. Barbatto, S. Borin, S. Licocchia, V. Garavaglia, F. Adani, Using olive mill wastewater to improve performance in producing electricity from domestic wastewater by using single-chamber microbial fuel cell, *Bioresour. Technol.* 147 (2013) 246–253.
- [57] A. Iannaci, B. Mecheri, A. D’Epifanio, M.J.L. Elorri, S. Licocchia, Iron–nitrogen-functionalized carbon as efficient oxygen reduction reaction electrocatalyst in microbial fuel cells, *Int. J. Hydrogen Energy* 41 (2016) 19637–19644.
- [58] F. Zen, M.D. Angione, J.A. Behan, R.J. Cullen, T. Duff, J.M. Vasconcelos, E.M. Scanlan, P.E. Colavita, Modulation of protein fouling and interfacial properties at carbon surfaces via immobilization of glycans using aryldiazonium chemistry, *Sci. Rep.* 6 (2016) 24840.
- [59] J.A. Behan, A. Myles, A. Iannaci, E. Whelan, E.M. Scanlan, P.E. Colavita, Bioinspired electro-permeable glycans at carbon: fouling control for sensing in complex matrices, *Carbon* 158 (2020) 519–526.
- [60] R.L. McCreery, Advanced carbon electrode materials for molecular electrochemistry, *Chem. Rev.* 108 (2008) 2646–2687.
- [61] P. Doppelt, G. Hallais, J. Pinson, F. Podvorica, S. Verneyre, Surface modification of conducting substrates. Existence of Azo bonds in the structure of organic layers obtained from diazonium salts, *Chem. Mater.* 19 (2007) 4570–4575.
- [62] J.K. Kariuki, M.T. McDermott, Nucleation and growth of functionalized aryl films on graphite electrodes, *Langmuir* 15 (1999) 6534–6540.
- [63] J.K. Kariuki, M.T. McDermott, Formation of multilayers on glassy carbon electrodes via the reduction of diazonium salts, *Langmuir* 17 (2001) 5947–5951.
- [64] M. Zhou, M. Chi, J. Luo, H. He, T. Jin, An overview of electrode materials in microbial fuel cells, *J. Power Sources* 196 (2011) 4427–4435.
- [65] A. Kumar, L.H.-H. Hsu, P. Kavanagh, F. Barrière, P.N. Lens, L. Lapinonnière, U. Schröder, X. Jiang, D. Leech, The ins and outs of microorganism–electrode electron transfer reactions, *Nat. Rev. Chem.* 1 (2017) 0024.
- [66] T. Kaplas, P. Kuzhir, Ultra-thin pyrocarbon films as a versatile coating material, *Nanoscale Res. Lett.* 12 (2017) 121.
- [67] C. Santoro, M. Guilizzoni, J.P. Correa Baena, U. Pasaogullari, A. Casalegno, B. Li, S. Babanova, K. Artyushkova, P. Atanassov, The effects of carbon electrode

- surface properties on bacteria attachment and start up time of microbial fuel cells, *Carbon* 67 (2014) 128–139.
- [68] Y.-R. He, X. Xiao, W.-W. Li, G.-P. Sheng, F.-F. Yan, H.-Q. Yu, H. Yuan, L.-J. Wu, Enhanced electricity production from microbial fuel cells with plasma-modified carbon paper anode, *Phys. Chem. Chem. Phys.* 14 (2012) 9966–9971.
- [69] S.-H. Chang, J.-S. Liou, J.-L. Liu, Y.-F. Chiu, C.-H. Xu, B.-Y. Chen, J.-Z. Chen, Feasibility study of surface-modified carbon cloth electrodes using atmospheric pressure plasma jets for microbial fuel cells, *J. Power Sources* 336 (2016) 99–106.
- [70] B.-Y. Chen, Y.-T. Tsao, S.-H. Chang, Cost-effective surface modification of carbon cloth electrodes for microbial fuel cells by candle soot coating, *Coatings* 8 (2018) 468.
- [71] X.-Y. Wu, F. Tong, T.-S. Song, X.-Y. Gao, J.-J. Xie, C.C. Zhou, L.-X. Zhang, P. Wei, Effect of zeolite-coated anode on the performance of microbial fuel cells, *J. Chem. Technol. Biotechnol.* 90 (2015) 87–92.
- [72] X. Zhang, X. Xia, I. Ivanov, X. Huang, B.E. Logan, Enhanced activated carbon cathode performance for microbial fuel cell by blending carbon black, *Environ. Sci. Technol.* 48 (2014) 2075–2081.
- [73] S. Cheng, H. Liu, B.E. Logan, Increased power generation in a continuous flow MFC with advective flow through the porous anode and reduced electrode spacing, *Environ. Sci. Technol.* 40 (2006) 2426–2432.
- [74] M.-T. Nguyen, B. Mecheri, A. D'Epifanio, T.P. Sciarria, F. Adani, S. Licocchia, Iron chelates as low-cost and effective electrocatalyst for oxygen reduction reaction in microbial fuel cells, *Int. J. Hydrogen Energy* 39 (2014) 6462–6469.
- [75] N. Pous, A.A. Carmona-Martínez, A. Vilajeliu-Pons, E. Fiset, L. Bañeras, E. Trably, M.D. Balaguer, J. Colprim, N. Bernet, S. Puig, Bidirectional microbial electron transfer: Switching an acetate oxidizing biofilm to nitrate reducing conditions, *Biosens. Bioelectron.* 75 (2016) 352–358.
- [76] B. Cercado, N. Byrne, M. Bertrand, D. Pocaznoi, M. Rimboud, W. Achouak, A. Bergel, Garden compost inoculum leads to microbial bioanodes with potential-independent characteristics, *Bioresour. Technol.* 134 (2013) 276–284.
- [77] L.E. Doyle, E. Marsili, Weak electricigens: A new avenue for bioelectrochemical research, *Bioresour. Technol.* 258 (2018) 354–364.
- [78] G.T. Kim, M.S. Hyun, I.S. Chang, H.J. Kim, H.S. Park, B.H. Kim, S.D. Kim, J.W.T. Wimpenny, A.J. Weightman, Dissimilatory Fe(III) reduction by an electrochemically active lactic acid bacterium phylogenetically related to *Enterococcus gallinarum* isolated from submerged soil, *J. Appl. Microbiol.* 99 (2005) 978–987.
- [79] K. Fricke, F. Harnisch, U. Schröder, On the use of cyclic voltammetry for the study of anodic electron transfer in microbial fuel cells, *Energy Environ. Sci.* 1 (2008) 144–147.
- [80] K.P. Katuri, P. Kavanagh, S. Rengaraj, D. Leech, *Geobacter sulfurreducens* biofilms developed under different growth conditions on glassy carbon electrodes: insights using cyclic voltammetry, *Chem. Commun.* 46 (2010) 4758–4760.
- [81] J.M. Vasconcelos, F. Zen, S.N. Stamatini, J.A. Behan, P.E. Colavita, Determination of surface ζ -potential and isoelectric point of carbon surfaces using tracer particle suspensions, *Surf. Interface Anal.* 49 (2017) 781–787.
- [82] C. Santoro, S. Babanova, K. Artyushkova, J.A. Cornejo, L. Ista, O. Bretschger, E. Marsili, P. Atanassov, A.J. Schuler, Influence of anode surface chemistry on microbial fuel cell operation, *Bioelectrochemistry* 106 (2015) 141–149.
- [83] K.-Y. Law, Definitions for hydrophilicity, hydrophobicity, and superhydrophobicity: getting the basics right, *J. Phys. Chem. Lett.* 5 (2014) 686–688.
- [84] R.J. Pieters, Intervention with bacterial adhesion by multivalent carbohydrates, *Med. Res. Rev.* 27 (2007) 796–816.